ELSEVIER

Journal of Fluids and Structures 18 (2003) 651–661

JOURNAL OF FLUIDS AND STRUCTURES

www.elsevier.nl/locate/jnlabr/yjfls

Self-excited vibration of cross-shaped tube bundle in cross-flow

F. Inada[a,*], T. Nishihara[b], A. Yasuo[a], R. Morita[a], A. Sakashita[c], J. Mizutani[c]

[a] *Nuclear Energy Systems Department, Central Research Institute of Electric Power Industry (CRIEPI), 2-11-1, Iwado-Kita, Komae-shi Tokyo 201-8511, Japan*

[b] *Central Research Institute of Electric Power Industry (CRIEPI), Dept. 1646, Abiko, Abiko-shi, Chiba 270-1194, Japan*

[c] *Tokyo Electric Power Company, 1-1-3 Uchisaiwai-cho, Chiyoda-ku, Tokyo 100-0011, Japan*

Received 5 October 2002; accepted 11 July 2003

Abstract

A cross-shaped tube bundle is proposed for the lower plenum structure in next-generation LWRs. The vibration response of the cross-shaped tube bundle in cross-flow has been measured in water tunnel tests. First, a small-scale test was conducted. Tests were conducted with 3×3 flexible tubes as well as a single flexible tube in a rigid tube bundle. The flexible tubes could vibrate in the lift, drag, and torsional directions. The effect of the arrangement of the tube bundle and the natural frequency ratio of translational and torsional vibrations were considered. Second, a large-scale test was conducted for only one case to check the effect of Reynolds number, in which the Reynolds number was 10 times larger than that of the small-scale test. In all the cases, large-amplitude vibration appeared when the flow velocity became larger than a critical value, and self-excited vibration was found to occur. The nondimensional critical gap velocity of the large-scale test agreed well with that of the small-scale test, which suggested that the effect of Reynolds number was not so large. A design guideline to prevent self-excited vibration is proposed for the cross-shaped tube bundle.

1. Introduction

A cross-shaped tube bundle is proposed for the lower plenum structure in next-generation LWRs. Many studies have been conducted on the flow-induced vibration of circular tube bundles, as reviewed in depth by Paidoussis (1982), Chen (1984,1987), Weaver and Fitzpatrick (1988), Blevins (1990), Pettigrew and Taylor (1991), and Au-Yang (2001). However, very few studies can be found regarding the flow-induced vibration of a cross-shaped tube bundle. Nishihara et al. (2002,2003) measured the local fluid excitation force acting on a cross-shaped tube bundle in water tunnel tests, which could be used to estimate the amplitude of turbulence-induced vibration.

In this study, the vibration response of a cross-shaped tube bundle was measured in water tunnel tests to clarify the characteristics of self-excited vibration. First, a small-scale test was conducted. Tests were conducted with 3×3 flexible tubes as well as a single flexible tube in a rigid tube bundle. The flexible tubes could vibrate in the lift, drag, and torsional directions. Two types of arrangement, normal and staggered, were considered. Two cases of the natural frequency ratio of translational and torsional vibrations were considered: one when the natural frequency of the translational mode was much lower than that of the torsional mode, and the other when the natural frequency of the torsional mode was slightly lower than that of the translational mode. Second, a large-scale test was conducted to check the effect of Reynolds number only for one case in which a single flexible tube was supported in a rigid tube bundle and the natural frequency of the torsional mode was slightly lower than that of the translational mode.

*Corresponding author. Tel.: +81-3-3480-2111; fax: +81-3-3480-2493.
E-mail address: inada@criepi.denken.or.jp (F. Inada).

0889-9746/$ - see front matter © 2003 Elsevier Ltd. All rights reserved.
doi:10.1016/j.jfluidstructs.2003.07.015

Nomenclature

C_{nB}	mass-damping parameter of translational mode
C_{nT}	mass-damping parameter of torsional mode
D	reference length of cross-shaped tube
f	the lowest natural frequency in water
I	inertia moment of cross-shaped tube per unit length
I_{aT}	added inertia moment per unit length
K_B	added mass coefficient
K_T	added inertia moment coefficient
m	mass of cross-shaped tube per unit length
M_{aB}	added mass per unit length
Re	Reynolds number ($= UD/v$)
U	gap velocity
U_{cr}	critical gap velocity
ζ	damping ratio
v	kinematic viscosity
ρ	density of fluid

2. Small-scale test

2.1. Experimental apparatus

Fig. 1 is a schematic diagram of the test loop of the small-scale test. Water is pumped from a water storage tank, flows through the turbine flow meter, surge tank, flow rectifier, and into a test section, in which water flows perpendicularly to the tube bundle. In the flow rectifier, the flow channel is partitioned by a lattice, where the width of each lattice is 5 cm, and the length of the flow rectifier is 50 cm. The turbulence intensity at the inlet of the test section was 6%, which was measured with a hot film at the entrance of the test section. The accuracy of the turbine flow meter was less than 5%. The water that flows out of the test section returns to the water storage tank.

Fig. 2 shows the arrangements of the cross-shaped tube bundle in the test section. Fig. 2(a) is the normal arrangement and Fig. 2(b) is the staggered arrangement. Nine tubes, that is, the 3×3 tube bundle colored gray in Fig. 2, are flexibly supported and can vibrate. The tubes colored black surrounding the flexible tube bundle are rigid. The reference length of the cross-shaped tube shown in Fig. 2 is around 90 mm, and the pitch of the tube bundle is 75 mm. The tubes are made of aluminum alloy. The mass of the tube per unit length is around 5 kg/m.

Fig. 3 shows the support structure of the flexible tubes. Fig. 3(a) is a cantilever tube, in which the cross-shaped tube is supported by a circular cylinder of 12 mm in diameter and 30 mm in length made of aluminum alloy. In this case, the natural frequency of the translational mode is much lower than that of the torsional mode, and self-excited vibration of the translational mode is expected to occur. To check the torsional mode, the tubes are supported at both ends by a slender circular cylinder of 4.5 mm in diameter and 80 mm in length as shown in Fig. 3(b), in which the natural

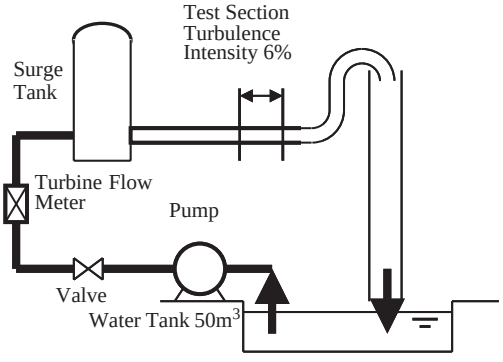

Fig. 1. Test loop of small-scale test.

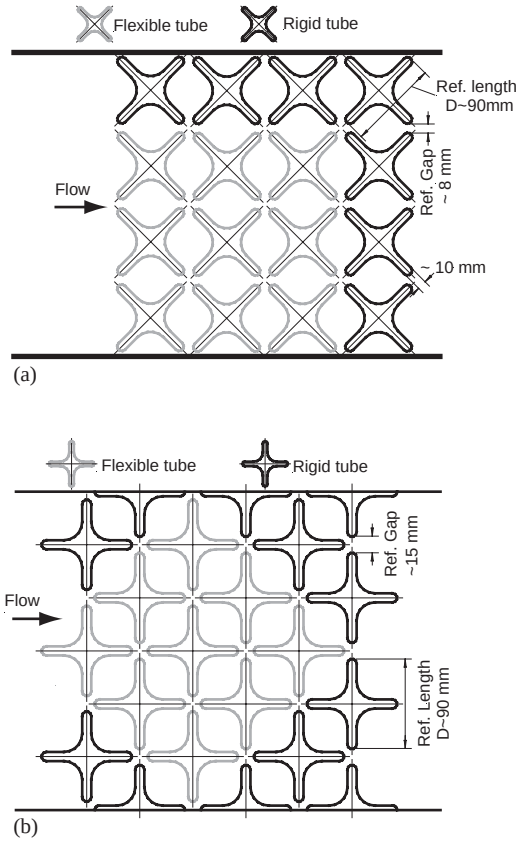

Fig. 2. Arrangements of the cross-shaped tube bundle in the test section and the location of flexible tubes when the test was conducted with the 3×3 flexible tube bundle: (a) normal arrangement and (b) staggered arrangement.

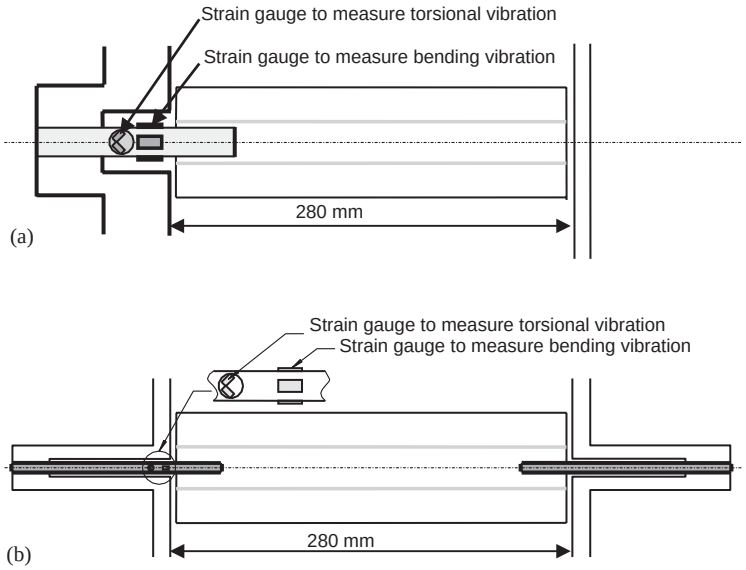

Fig. 3. Support structure of flexible tubes in the small-scale test: (a) cantilever tube and (b) tube supported at both ends.

frequency of the torsional mode is slightly lower than that of the translational mode. In this case, the experiment is conducted only for the normal arrangement.

Translational and torsional displacements are measured by strain gauges as shown in Fig. 3. To calibrate the strain gauges, the load was applied to the rod edge before the rod was assembled, and it was checked that the relation between the strain and the load satisfied the equation of beam bending.

In the data acquisition, the sampling frequency was 640 Hz, and 131,072 samples ($\sim$3.4 min) were collected for one experimental condition to obtain the root mean square (r.m.s.) value of tube displacement.

The static offset due to gravity was estimated using the NASTRAN code, which yielded the value of 0.2 mm for the cantilevered tube and 0.17 mm for the tube with both ends fixed, which were much smaller than the gap, so the static offset was ignored in this study.

2.2. Added mass and mass-damping parameter

The impulse response was measured with a hammer. An example of the power spectral density of tube displacement is shown in Fig. 4. Figs. 4(a) and (b) show the result in air and water, respectively. In air, there was a single sharp peak and so the natural frequency could be obtained easily. However, in water, there were many peaks, which may have been because of many coupled modes of the tube bundle. Since it is a 3×3 flexible tube bundle, there can be 27 coupled modes. In order to extrapolate the experimental results to reactor design, we need to nondimensionalize the results of vibration response, and to derive a single added mass coefficient. This requires a single reference natural frequency in water.

We therefore conducted an impact test for the case of a single flexible tube in a rigid tube bundle. The center tube of the tubes colored gray in Fig. 2 was flexible. The result is shown in Fig. 4(c). There was a single sharp peak because there was no coupling among tubes, and so from this figure we could obtain a single reference natural frequency in water.

The natural frequency in water shown in Fig. 4(c) was lower than that in air because of the large added mass.

The added mass and added inertia moment coefficients, K_B and K_T, which are defined as

$$M_{aB} = K_B \frac{1}{4}\rho\pi D^2, \quad I_{aT} = K_T \frac{1}{128}\rho\pi D^4 \tag{1}$$

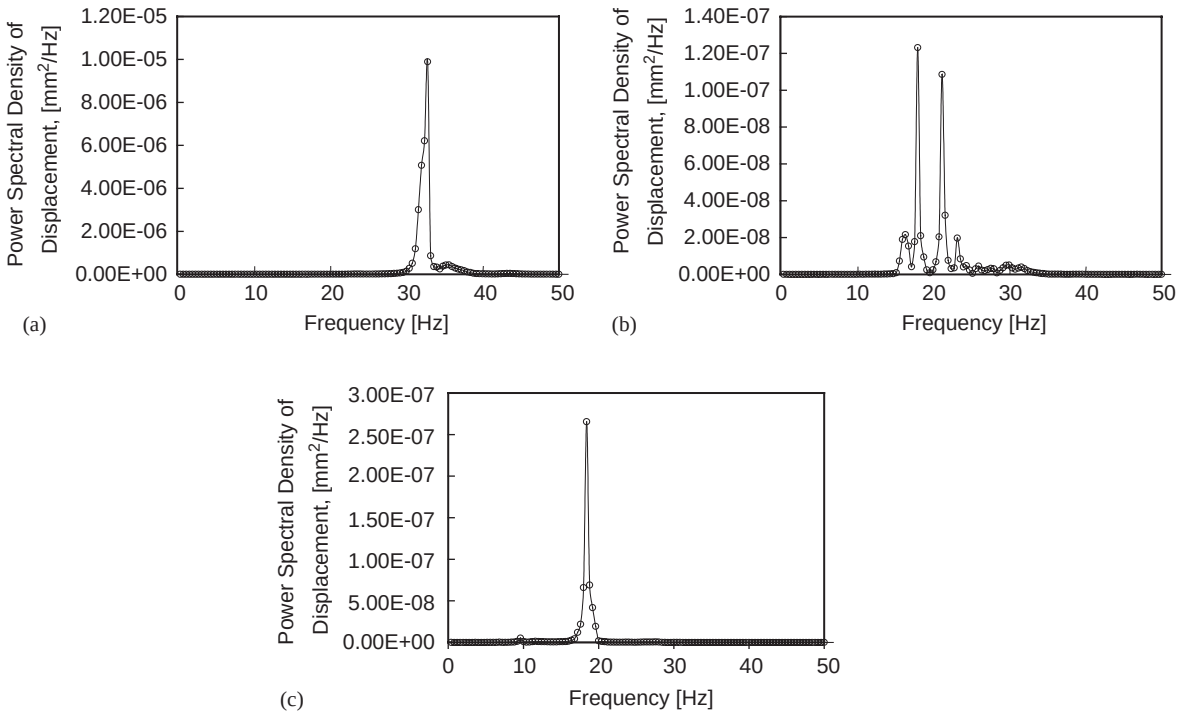

Fig. 4. Power spectral density of impact response of cantilever flexible tubes: In the case of (a) 3×3 flexible tube bundle in air; (b) 3×3 flexible tube bundle in water; (c) single flexible tube in rigid tube bundle in water.

Table 1
Summary of impact response of small-scale test

		Cantilever	Both ends supported
Natural freq. in air	Bending mode	33	44
	Torsional mode	204	29
Natural freq. in water	Bending mode	19	24
	Torsional mode	151	22
K_B, K_T		$K_B = 1.7$, $K_T = 1.5$	$K_B = 1.8$, $K_T = 1.5$
Damping ratio in water	Bending mode	0.015	
	Torsional mode		0.018
Mass-damping parameter	Bending mode	0.056	
	Torsional mode		0.0051

were obtained by using the natural frequencies in water and in air where the reference natural frequency was obtained in the case of the single flexible tube in the rigid tube bundle. The result is shown in Table 1. If the added mass is the same as that of a plate of the same reference length, K_B and K_T become unity. Table 1 shows that K_B and K_T were larger than unity because of the effect of confinement of the tube bundle.

Mass-damping parameters of the translational and torsional modes defined by

$$C_{nB} = \frac{2\pi\zeta m}{\rho D^2}, \quad C_{nT} = \frac{2\pi\zeta I}{\rho D^4} \tag{2}$$

were obtained for the single flexible tube in the rigid tube bundle in water, which is also shown in Table 1 where m and I are the mass and the inertia moment of the cross-shaped tube per unit length.

2.3. Results of self-excited vibration tests

Fig. 5 shows the results for the normal arrangement with the tubes cantilever mounted. The natural frequency of the translational mode was much smaller than that of the torsional mode. The amplitude of tube vibration, that is, the r.m.s. value of displacement, is shown as a function of nondimensional gap velocity U/fD in Fig. 5(a), where the amplitude of torsional vibration is expressed in terms of tip vibration displacement of the cross-shaped tube [$= D\theta/2$, θ: torsional displacement of the tube in angle (rad)]. The gap velocity is the averaged flow velocity at the reference gap in Fig. 2(a), which is the total flow rate divided by the flow area at the gap. The amplitude of the translational mode was small in the range of $U/fD < 0.26$, and it rapidly became large when U/fD increased above 0.27, and it was found that self-excited vibration occurred. A conservative value of the nondimensional critical gap velocity U_{cr}/fD of 0.26 was obtained, which was the experimental condition just before large amplitude vibration occurred. The Reynolds number $\mathrm{Re} = U_{cr}D/\nu$ at the critical gap velocity was 3.5×10^4, which is 1/70 of that of a typical next-generation reactor. When large amplitude vibration occurred and U/fD was smaller than 0.35, the amplitude of vibration in the lift direction was much larger than that in the drag direction. When U/fD increased above 0.35, the amplitude of vibration in the drag direction also became large. The amplitude of torsional vibration was very small.

The nondimensional critical gap velocity U_{cr}/fD of the cross-shaped tube bundle was around 1/10 of that of the circular tube bundle, which is at least above unity when the mass-damping parameter ranges from 10^{-2} to 10^0 (Chen, 1989). This could be because (1) reference length D was large and U_{cr}/fD looked small, and (2) the tubes were arranged very closely, and self-excited vibration could easily occur because of the coupling of tubes.

Fig. 5(b) shows the frequency of large amplitude vibration as a function of U/fD. When U/fD was below 0.35, in which the amplitude of vibration in the drag direction was small, the vibration frequency almost coincided with the natural frequency of the translational mode in the case of the single flexible tube in the rigid tube bundle in water. This mode was called "Mode A". For $U/fD > 0.35$, the frequency was smaller than the natural frequency of the translational mode of the single flexible cylinder in water. This mode was called "Mode B".

Fig. 5(c) shows an example of the vibration modes of Mode A and B. Though the tubes of the 3×3 tube bundle were flexibly supported, the trajectory of translational vibration is shown for the center tube as well as its four adjacent tubes.

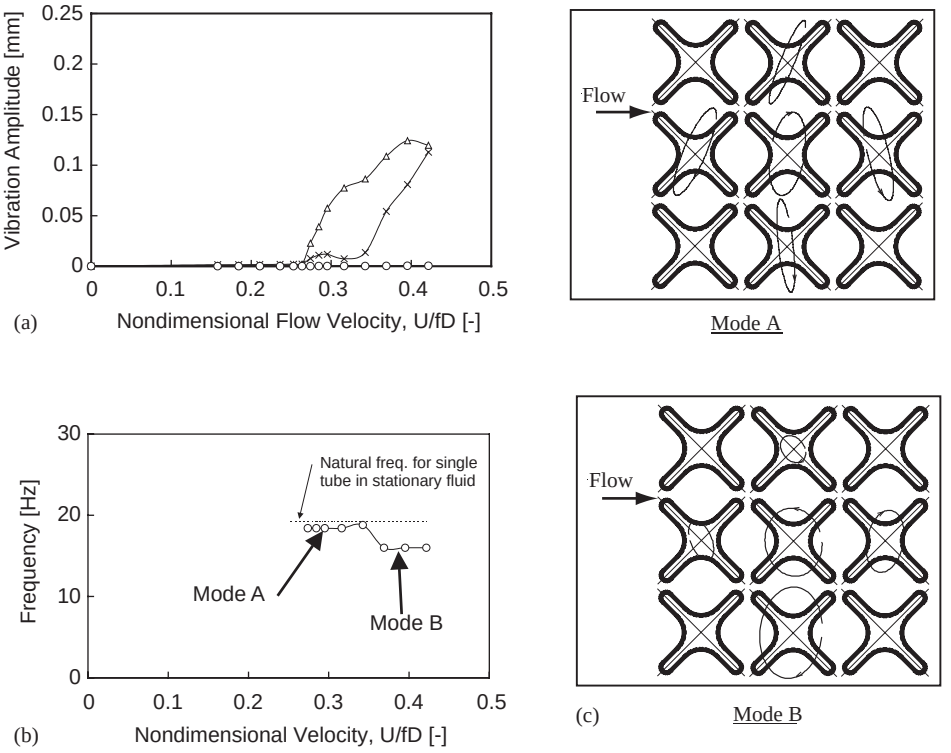

Fig. 5. Vibration response of normal arrangement in the case of 3×3 cantilever flexible tubes: (a) r.m.s. value of displacement as a function of nondimensional gap flow velocity, (○) torsional mode, (Δ) lift direction, (x) drag direction; (b) vibration frequency of large amplitude vibration; and (c) examples of vibration mode.

For Mode A, the amplitude of vibration in the lift direction was much larger than that in the drag direction. For vibration in the lift direction, the phase of the center tube was opposite to that of the four adjacent tubes.

On the other hand, for Mode B, the amplitude of vibration in the drag direction was similar to that in the lift direction. For vibration in the lift direction, the phase of the upper and lower tubes was opposite to that of the center tube, but the phase of the left and right tubes was almost the same as that of the center tube. Therefore, the change of frequency at $U/fD = 0.35$ could be because of the change of mode.

Fig. 6 shows the result for the staggered arrangement. The gap velocity was obtained as the averaged flow velocity at the reference gap in Fig. 2(b), which is the total flow rate divided by the flow area at the gap. The nondimensional critical gap velocity was 0.3 as shown in Fig. 6(a), which was slightly larger than U_{cr}/fD of the normal arrangement. The vibration frequency was lower than the natural frequency in the case of the single flexible tube in the rigid tube bundle in water (see Fig. 6(b)). The trajectory of translational mode vibration inclined by 45° as shown in Fig. 6(c).

Fig. 7 shows the result when the flexible tubes are fixed at both ends as shown in Fig. 3(b) and the natural frequency of the torsional mode is slightly lower than that of the translational mode. The vibration mode was torsional. Note that translational mode vibration occurred in Figs. 5 and 6 because cantilever tubes were used for the flexible tube, and the natural frequency of the translational mode was much smaller than that of the torsional mode. The arrangement was the normal arrangement. The nondimensional critical gap velocity was around 0.24 (see Fig. 7(a)), where the reference frequency was defined as the natural frequency of the torsional mode when the vibration mode was torsional. The frequency was close to the natural frequency of the torsional mode for the case of the single flexible tube in the rigid tube bundle in water (see Fig. 7(b)). The phase of the center tube was opposite to that of the upper and lower tubes, and is the same as that of the right and left tubes (see Fig. 7(c)).

Fig. 8 shows the result when the single flexible tube was supported at both ends in the rigid tube bundle. The nondimensional critical gap velocity was 0.3, and the mode of large amplitude vibration was torsional. The result will be compared with that of the large-scale test mentioned in the next section to check the effect of Reynolds number.

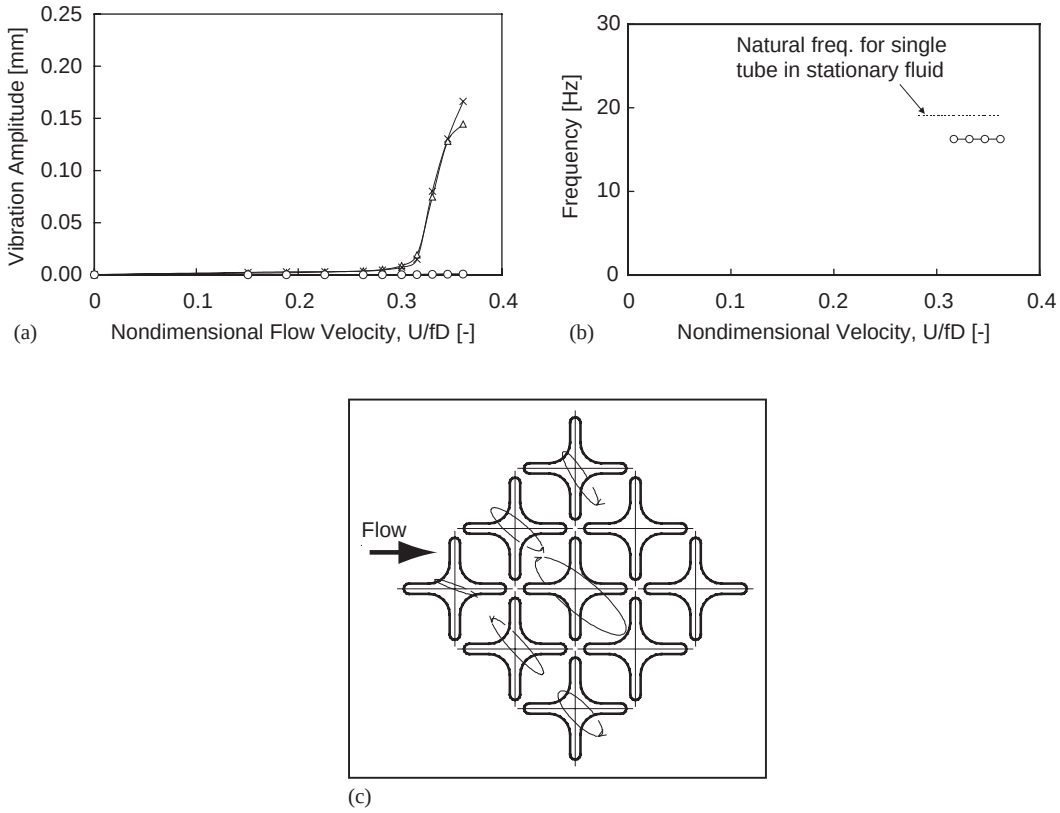

Fig. 6. Vibration response of staggered arrangement in the case of 3×3 cantilever flexible tubes: (a) r.m.s. value of displacement as a function of nondimensional gap flow velocity, (○) torsional mode, (Δ) lift direction, (x) drag direction; (b) vibration frequency of large amplitude vibration; and (c) examples of vibration mode.

3. Large-scale test

3.1. Large-scale test loop

The test loop for the large-scale test with a large head tank in the Abiko Laboratory of CRIEPI shown in Fig. 9 was used. The loop has a head tank of 5 m in diameter, and the water stored in the tank falls by gravity through a test section of 0.5×1 m. The flow velocity can be controlled by the exit control valve. The flow velocity was measured by an electromagnetic flow probe installed upstream of the test section, which was calibrated by the descent rate of the water level of the head tank. The turbulence intensity at the inlet of the test-section was 1.5%.

3.2. Test section of large-scale test

The test-section is shown in Fig. 10. The test was conducted for only one case, that is, the tube bundle was the normal arrangement, in which a single tube was supported at both ends in the rigid tube bundle. The support sections were circular, made of aluminum alloy, and measured 24 mm in inside diameter, 31 mm in outside diameter, and 100 mm in length. The scale of the reference length of the cross-shaped tube, D, as well as the spacing among tubes were scaled up by a factor of 2.2. D was around 200 mm and P was around 20 mm. The mass per unit length of the tube was around 22 kg/m. The length of the cross-shaped tube was 1 m. The tubes were made of aluminum alloy. The displacement of vibration was measured with strain gauges for both torsional and translational vibration. To calibrate the strain gauges, the load was applied to the cross-shaped tube, and the relation between the strain and the load was analyzed.

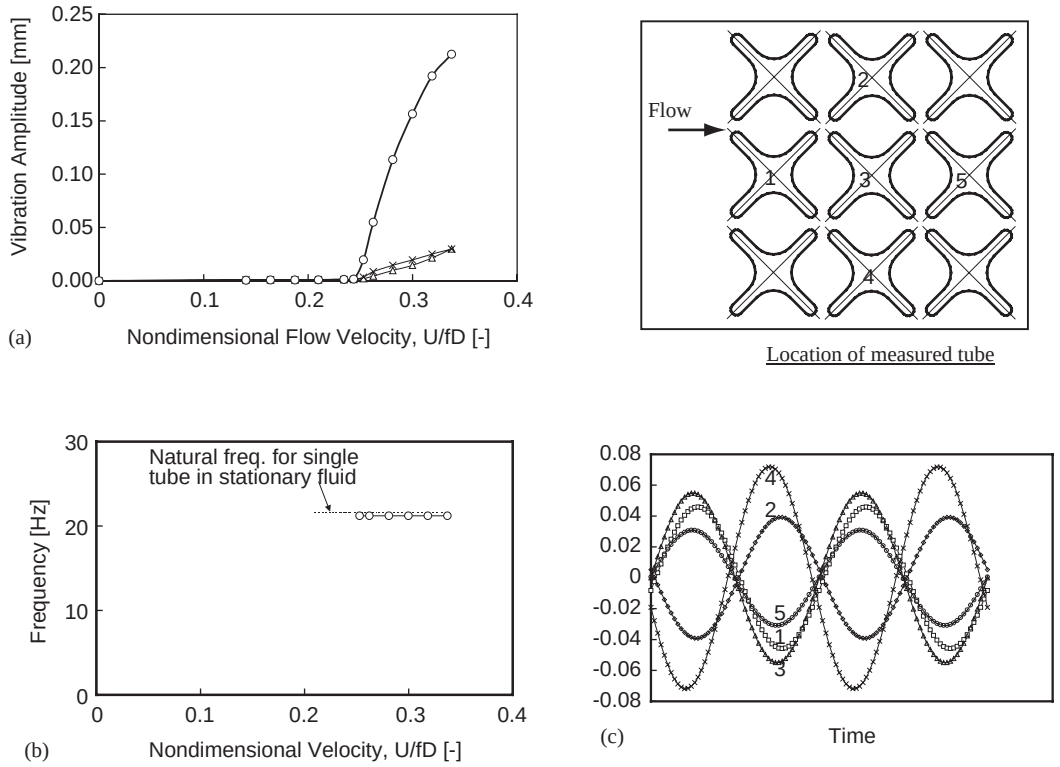

Fig. 7. Vibration response of normal arrangement in the case of 3×3 flexible tubes supported at both ends: (a) r.m.s. value of displacement as a function of nondimensional gap flow velocity, (○) torsional mode, (Δ) lift direction, (x) drag direction; (b) vibration frequency of large amplitude vibration; and (c) examples of vibration mode.

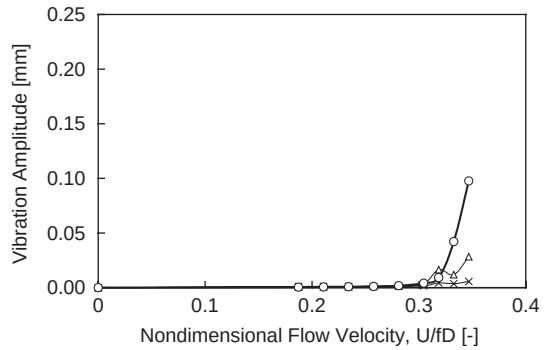

Fig. 8. R.m.s. value of displacement as a function of nondimensional gap flow velocity in the case of normal arrangement and single flexible tube supported at both ends in rigid tube bundle: (○) torsional mode; (Δ) lift direction; (x) drag direction.

3.3. Added mass and mass-damping parameter

The impulse response was obtained with a hammer. The natural frequency in water and air were obtained, from which the added mass coefficient and added inertia moment coefficient were calculated. The damping coefficients of torsional and translational modes were estimated by applying the half power method to the power spectral density of impulse response. The mass-damping parameter of the torsional mode was also calculated. The results are summarized in Table 2.

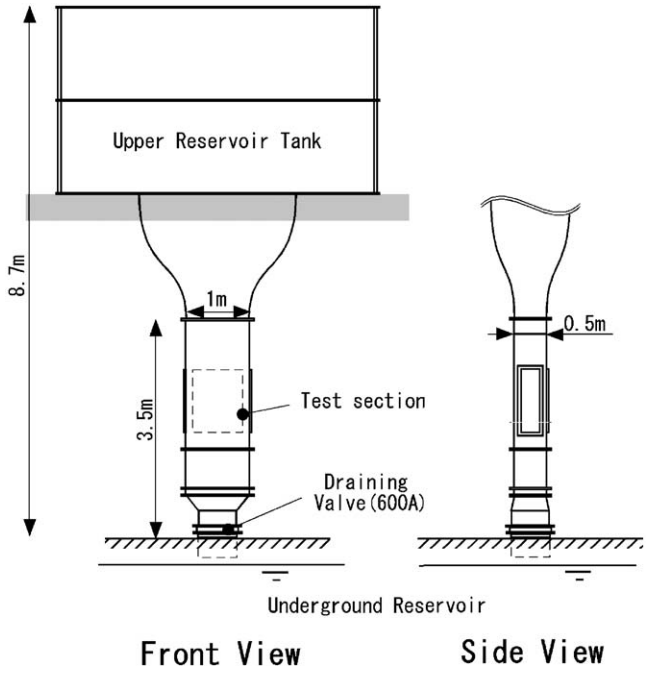

Fig. 9. Test loop for large-scale test with large head tank in Abiko Laboratory of CRIEPI.

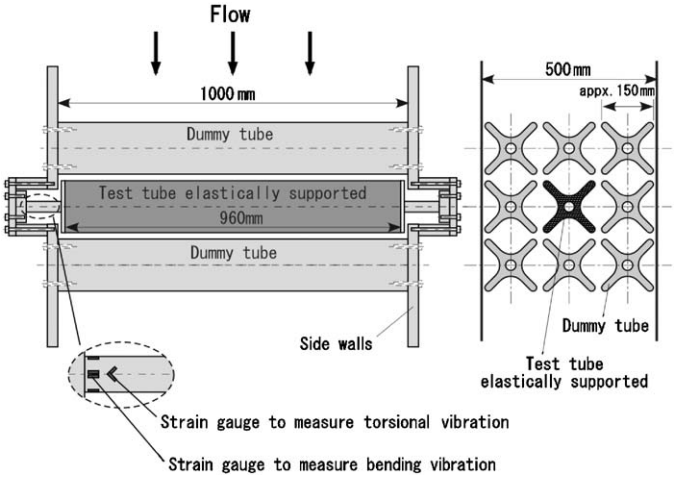

Fig. 10. Test section of large-scale test.

Added mass coefficient K_B of the large-scale test was 15% larger than that of the small-scale test, and added inertia moment coefficient K_T was 7% smaller than that of the small-scale test. The results of the large- and small-scale tests were very similar to each other.

The damping ratio in water was 0.2%, which was very small, and the mass-damping parameter of torsional vibration was 0.00056, which was 1/10 of that of the small-scale test under the same support conditions (see Table 1).

Next, we consider the effect of the mass-damping parameter in the tube bundle of the circular cylinder. When the mass-damping parameter is much smaller than unity, fluid force is dominant, and the mass-damping parameter has little effect. The concept might be the same in the case of the cross-shaped tube bundle. Although we cannot conclude the effect of the mass-damping parameter on U_{cr}/fD of the cross-shaped tube bundle at this stage, as a preliminary

evaluation we can assume that the effect of the mass-damping parameter on the critical velocity is not so large. If the tube bundle is in a fluid of low density, the mass-damping parameter becomes large, and the nondimensional critical velocity depends highly on the mass-damping parameter.

3.4. Results of self-excited vibration in large-scale test

Fig. 11 shows the r.m.s. value of vibration displacement as a function of U/fD. The flexible tube vibrated in the torsional direction. The nondimensional critical velocity was compared with that of the small-scale test (see Fig. 8) in Table 3, and the values agreed very well with each other. At the critical velocity, Reynolds number was also compared as shown in Table 3. The Reynolds number of the large-scale test was 10 times larger than that of the small-scale test, suggesting that the effect of Reynolds number was not so large when Reynolds number was below 10^6.

Now, let us consider the effect of Reynolds number on the single circular cylinder. In this case, Strouhal number is almost constant when $\mathrm{Re} < 3 \times 10^5$, but when $\mathrm{Re} > 3 \times 10^5$, the number changes. This is because the separation point changes. In the case of the cross-shaped tube, the separation point might not change as much, and so the effect of Reynolds number would not be so large.

Table 2
Summary of impact response of large-scale test

Natural freq. in air	Bending mode	145
	Torsional mode	95
Natural freq. in water	Bending mode	76
	Torsional mode	72
K_B, K_T		$K_B = 1.9$, $K_T = 1.4$
Damping ratio in water	Torsional mode	0.002
Mass-damping parameter	Torsional mode	0.00056

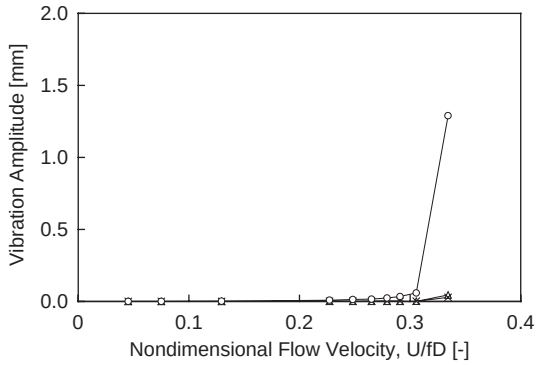

Fig. 11. R.m.s. value of displacement in the case of large-scale test: (○) torsional mode; (Δ) lift direction; (x) drag direction.

Table 3
Reynolds number and nondimensional critical velocity of small- and large-scale test

	Small-scale test	Large-scale test
Re	6.2×10^4	6.8×10^5
U_{cr}/fD	0.3	0.3

4. Design guideline

We now consider the case where the cross-shaped tube bundle is designed for a lower plenum structure, in which the natural frequency of the translational mode is much lower than that of the torsional mode. The nondimensional critical gap velocity of the normal arrangement was slightly smaller than that of the staggered arrangement, so if we use U_{cr}/fD of the normal arrangement, the evaluation becomes conservative. Moreover, from the CFD calculation in the lower plenum, the cross-flow component was found to be larger for the interior tubes than the upstream tubes, and the fluid flowed like the normal arrangement for the interior tubes. For the large-scale structure, if Reynolds number is below 10^6, the effect of Re is probably small. Even if the Reynolds number is above 10^6, the effect might be not so large, but further consideration on the effect of Reynolds number is needed.

5. Conclusions

The vibration response of a cross-shaped tube bundle in cross-flow was estimated experimentally.

1. Large-amplitude vibration appeared when the flow velocity exceeded a critical value, and self-excited vibration was found to occur.
2. The nondimensional critical gap velocity of the normal arrangement was slightly smaller than that of the staggered arrangement.
3. When the natural frequency of the translational mode was much lower than that of the torsional mode, self-excited vibration of the translational mode occurred, and when that of the torsional mode was slightly lower than that of the translational mode, self-excited vibration of the torsional mode occurred.
4. The effect of Reynolds number on the nondimensional gap velocity was suggested to be not so large in the range of $\mathrm{Re} < 10^6$ because the result of the large-scale test agreed with that of the small-scale test when a single flexible tube was supported in a rigid tube bundle.

References

Au-Yang, M.K., 2001. Flow-Induced Vibration of Power and Process Plant Components, A Practical Workbook. ASME Press, New York.

Blevins, R.D., 1990. Flow Induced Vibration 2nd Edition. Krieger Publishing Company, New York.

Chen, S.S., 1984. Guidelines for the instability flow velocity of tube arrays in cross-flow. Journal of Sound and Vibration 98, 439–455.

Chen, S.S., 1987. Flow-Induced Vibration of Circular Cylindrical Structures. Hemisphere Publishing Corporation, Washington, DC.

Nishihara, T., Inada, F., Yasuo, A., Morita, R., Sakashita, A.Mizutani, J., 2002. Turbulence-induced fluid dynamic forces acting on cross-shaped tube bundle in cross flow. Proceeding of the Fifth International Symposium on FSI, Aeroelasticity & FIV + Noise. ASME, New York.

Nishihara, T., Inada, F., Yasuo, A., Morita, R., Sakashita, A., Mizutani, J., 2003. Turbulence-induced fluid dynamic forces acting on cross-shaped tube bundle in cross flow. Journal of Fluids and Structures 18, 635–650.

Paidoussis, M.P., 1982. A review of flow induced vibrations in reactors and reactor components. Nuclear Engineering and Design 74, 31–60.

Pettigrew, M.J., Taylor, C.E., 1991. Fluidelastic instability of heat exchanger tube bundles: review and design recommendations. ASME Journal of Pressure Vessel Technology 113, 242–256.

Weaver, D.S., Fitzpatrick, J.A., 1988. A review of cross-flow induced vibrations in heat exchanger tube arrays. Journal of Fluids and Structures 2, 73–93.